

Self-distillation with Online Diffusion on Batch Manifolds Improves Deep Metric Learning

Zelong Zeng
The University of Tokyo
& National Institute of Informatics
zzlbz@nii.ac.jp

Hong Liu
National Institute of Informatics
hliu@nii.ac.jp

Fan Yang
National Institute of Informatics
yang@nii.ac.jp

Shin'ichi Satoh
National Institute of Informatics
& The University of Tokyo
satoh@nii.ac.jp

November 15, 2022

Abstract

Recent deep metric learning (DML) methods typically leverage solely class labels to keep positive samples far away from negative ones. However, this type of method normally ignores the crucial knowledge hidden in the data (e.g., intra-class information variation), which is harmful to the generalization of the trained model. To alleviate this problem, in this paper we propose Online Batch Diffusion-based Self-Distillation (OBD-SD) for DML. Specifically, we first propose a simple but effective Progressive Self-Distillation (PSD), which distills the knowledge progressively from the model itself during training. The soft distance targets achieved by PSD can present richer relational information among samples, which is beneficial for the diversity of embedding representations. Then, we extend PSD with an Online Batch Diffusion Process (OBDP), which is to capture the local geometric structure of manifolds in each batch, so that it can reveal the intrinsic relationships among samples in the batch and produce better soft distance targets. Note that our OBDP is able to restore the insufficient manifold relationships obtained by the original PSD and achieve sig-

nificant performance improvement. Our OBD-SD is a flexible framework that can be integrated into state-of-the-art (SOTA) DML methods. Extensive experiments on various benchmarks, namely CUB200, CARS196, and Stanford Online Products, demonstrate that our OBD-SD consistently improves the performance of the existing DML methods on multiple datasets with negligible additional training time, achieving very competitive results. Code: https://github.com/ZelongZeng/OBD-SD_Pytorch

1 Introduction

Deep Metric Learning (DML) aims to learn an embedding space that uses predefined distance metrics (e.g., Euclidean distance) to reasonably measure the similarity between training samples and then transfer to unseen test data. The generalization capability of embedding space is very essential for many downstream applications of DML, such as image retrieval [8, 9], face recognition [38, 4], person re-identification [48, 12] and representation learning [47].

Most existing DML methods utilize a pre-defined

distance metric, depending on the class label, to increase the inter-class distance in the embedding space while decreasing the intra-class distance [41]. Typically, these methods promote intra-class samples to form a compact cluster with a large margin from other clusters, thus learning a strongly discriminative representation for the seen class, but ignoring the intrinsic relationships of the samples, such as intra-class variation. In particular, since the relationships of samples in the embedding space are derived solely from the distance metric based on the class labels, the diversity of the relationships of samples in the embedding space is suppressed. However, ignoring the intrinsic relationships of the samples actually harms the generalization of learned embedding space since they are useful to identify unseen classes [37, 26, 50, 57, 56].

To enhance this diversity, we propose a simple yet effective method called *Online Batch Diffusion-based Self-distillation* (OBD-SD), which is composed of two complementary components. Specifically, inspired by recent typical knowledge distillation techniques [6, 53, 19, 52], we first propose Progressive Self-distillation (PSD) that can be integrated into many typical DML methods [49, 46, 35]. For PSD, we define the student model trained in the previous epoch as the teacher model, which means that the student model serves as its own teacher model. This procedure does not require any modifications to the network architecture and incurs no further computational cost. In other words, in a dynamic manner, PSD distills the distance metric from the model at the previous epoch and then adaptively assigns a soft distance target for each training pair of data. We theoretically and experimentally analyze that the soft distance targets learned from PSD have more information about how the training samples are related to each other (rather than only considering the class label information). This helps to learn more diverse embedding representations and solves the problem described above.

It’s worth noting that a better distance metric should consider the local geometric structure of manifolds, rather than just using the rigid distance metrics, which is disregarded by our proposed PSD. Therefore, inspired by existing diffusion pro-

cess methods [59, 1, 51], we use the diffusion process to refine the distance target provided by the teacher model of PSD. We further proposed an Online Batch Diffusion Process (OBDP) technique, which aims to capture the local geometry structure of manifolds in a mini-batch. Our OBDP is able to learn the high-order information from batch manifolds, which presents the intrinsic relationships between samples and makes the soft distance targets more accurate. Note that, our OBDP makes use of a mini-batch to construct the manifold structure, which belongs to the online learning scheme, thereby significantly enhancing the computational efficiency. Our experiments and observations show that, compared with the existing methods doing diffusion on the global manifolds, this online learning scheme can achieve competitive or even better results.

We reformulate our OBD-SD model combining PSD and OBDP. The OBD-SD is a plug-and-play technique that can be integrated into most conventional DML methods with negligible extra computation cost. Our theoretical studies (as presented in Section 4) reveal that our OBD-SD can take into account the high-order relationship of samples, especially for hard samples. That is, our OBD-SD can learn a more accurate distance metric, which benefits the overall performance.

Finally, we conduct extensive experiments on three widely-used DML benchmarks, *i.e.*, CUB200-2011 [44], CARS196 [23] and Stanford Online Products [28], on which the results validate the merits of the proposed OBD-SD over the state-of-the-art (SOTA) DML methods. Moreover, experiments in Section 5.6 indicate that our OBD-SD indeed makes the learned embedding features achieve higher diversity and mitigate over-clustering [34], both encouraging better generalization to unseen test classes.

2 Related Works

2.1 Deep Metric Learning

Metric learning aims to learn a good metric space, in which we can measure the similarity between samples by using distance metrics. Recent works

leverage deep learning techniques to facilitate a better distance metric, which is called deep metric learning (DML). The pioneering works consider the relationship between a tuple of samples, such as pairs [10], triplets [45, 38, 49], and other variants (like N-pairs [40] and lifted structured loss [28]). Recently, AP-based losses [3, 31] and proxy-based methods [27, 29, 20] have demonstrated the capacity to learn distance-preserving embedding spaces. In addition, many different sampling schemes have been introduced to reduce the computational complexity caused by a large number of training pairs [38, 49, 7, 32, 33].

Recently, a promising direction is to explore how to learn a discriminative embedding space with good generalization to unseen classes. Most existing methods of this type consider learning an ensemble of embeddings by manually designing different learning objectives or constraints and demonstrate that the diversity of embedding representations is crucial to the generalization of embedding space [37, 32, 26, 50, 57, 56]. However, they usually face the problem of less scalability and high computational complexity. In contrast, our OBD-SD is efficient and straightforward, showing good scalability and generalization capabilities.

2.2 Knowledge Distillation

Early knowledge distillation (KD) attempts to compress models by transferring the “dark knowledge” from the larger teacher model to a compact student model [13, 54, 42]. Many recent works find that the student model can outperform the teacher model when the student is configured with the same capacity as its teacher [6, 52]. Based on this observation, they introduce a novel self-distillation (Self-KD) scheme. In addition, some other works, such as PS-KD [19], BYOT [55], and CS-KD [53], present a more effective and efficient simultaneous Self-KD scheme.

More recently, researchers begin to apply the Self-KD for improving the generalization of DML, taking RCL [21], BAR [30], and S2SD [34] as representative works. BAR applies the conventional strategy, *i.e.*, using a pre-trained model as the teacher. And S2SD extends DML with knowledge distillation from mul-

tiply auxiliary heads with high-dimension, all auxiliary heads share the same backbone with the base networks so they can be trained simultaneously. It’s worth noting that our work is somewhat similar to S2SD. We elaborate on some major differences between S2SD and ours as follows: First, S2SD targets the task of “feature compression”, *i.e.*, using high-dimensional embedding space with better generalization capacity to assist the training of low-dimensional embedding space. In contrast, Our OBD-SD proposes that the same dimensional embedding (as opposed to the high-dimensional embedding of S2SD) space itself can provide helpful information to improve performance, while S2SD does not. Second, our OBD-SD proposes Online Batch Diffusion Process (OBDP) for refining soft distance targets from the teacher. We also apply our OBDP to the existing Self-KD-based methods, and the experiments in Section 5.4 show that our OBDP can significantly improve the performance of the compared Self-KD-based DML methods.

2.3 Diffusion Process

The diffusion process is commonly used as a re-ranking method in retrieval tasks [59, 5, 1, 16, 51]. Due to the diversity of data, there is usually a distribution difference between training data and unknown test data [39]. The difference often results in manifolds in the embedding space that are not conducive to measuring the relationships between test samples using the rigid distance metric [51]. To handle this problem, diffusion process can capture the local geometry structure of the data manifolds based on a neighborhood graph, which can make distance metric more accurately [1]. Such a neighborhood graph consists of various nodes and edges, where each node represents a feature from the database and the edge presents the connection between each node and its neighborhood with corresponding weights proportional to the pairwise affinities between nodes. Additionally, diffusion process is often applied in label propagation for deep semi-supervised learning [58, 15, 14]. Different from these diffusion process methods proposed as the post-processing method, our OBD-SD uses diffusion process as an auxiliary

module that can refine the soft distance targets well during the training. Moreover, our OBD-SD uses only the mini-batch data for each diffusion process, which is more efficient than the conventional methods of using global data.

3 Proposed Method

3.1 Problem Formulation

For metric learning, we denote $\mathcal{X} = \{\mathbf{x}_1, \mathbf{x}_2, \dots, \mathbf{x}_n\}$ as the training data, and y_i is the corresponding label of \mathbf{x}_i . Our goal is to learn an embedding function $f : \mathcal{X} \mapsto \Phi \subset \mathbb{R}^d$ that maps each input $\mathbf{x} \in \mathcal{X}$ to the d -dimensional embedding space Φ that allows measuring the similarity between inputs. To this end, Let f be formulated as a differentiable deep network $f(\cdot, \theta)$ with a trainable parameter θ . The output $\mathbf{v}_i = f(\mathbf{x}_i, \theta)$ is typically normalized to $\mathbf{z}_i = \frac{\mathbf{v}_i}{\|\mathbf{v}_i\|}$. The distance (or similarity) between two inputs $\mathbf{x}_i, \mathbf{x}_j$ in the learned metric space is defined as $D_{i,j} := d(\mathbf{z}_i, \mathbf{z}_j)$, where $d(\cdot, \cdot)$ is the pre-defined distance (or similarity) function. In this paper, we use cosine similarity as the default, *i.e.*, $D_{i,j} = \mathbf{z}_i \cdot \mathbf{z}_j$.

3.2 Progressive Self-distillation

In this paper, we aim to solve the problem of ignoring the intrinsic relationships, so that a feasible way is to assign a more precise distance target for each pair. However, we usually only have the class labels of the data with the lack of characteristic annotations (e.g., attribute labels), which makes current DML difficult to get actual distance targets only by the annotation of the samples. Inspired by previous works [6, 30], we exploit knowledge distillation strategy to obtain soft distance targets from a teacher model.

To achieve this goal, the first problem we need to solve is how to obtain the teacher model. Previous works usually use a pre-trained model [30, 21] or add auxiliary architecture [34] as the teacher model. However, these methods are inflexible and require a longer training time.

An interesting observation [52] is that a relatively poorly-trained teacher model can still help improve

the student model. Inspired by this, we proposed a Progressive Self-distillation (PSD), which dynamically exploits the model trained in the previous epoch as the teacher model. In special, when finishing the training of the model in epoch $(t - 1)$, we copy and freeze this model as the teacher model used in the next epoch, which is defined as $f^{(T)}$. When we continue to train the student model $f^{(S)}$ in the epoch (t) , we use the $f^{(T)}$ to provide soft distance targets for knowledge distillation.

Then, the second problem is how to design the knowledge distillation loss function. Similar to previous works [30, 34], PSD matches sample relationships within a mini-batch \mathcal{B} in base space and target space, which can ensure the generality of the KD functions while fully utilizing the information of samples in the batch. Specifically, we calculate the similarity matrix $D \in \mathbb{R}^{|\mathcal{B}| \times |\mathcal{B}|}$, where $D_{i,j}$ indicates the cosine similarity between i -th and j -th sample in the mini-batch \mathcal{B} . Then, we use KL divergence as the basic of our PSD loss, which is shown as:

$$L_{\text{PSD}}(\mathcal{B}) = \frac{1}{|\mathcal{B}|} \sum_{i=1}^{|\mathcal{B}|} \sum_{j=1}^{|\mathcal{B}|} \sigma(D_{i,:}^{(T)}/\tau)_j \ln \frac{\sigma(D_{i,:}^{(T)}/\tau)_j}{\sigma(D_{i,:}^{(S)}/\tau)_j}, \quad (1)$$

where $\sigma()$ is the softmax operation, τ is a temperature parameter, $D_{i,:}$ indicates the i -th row of the matrix D , and $D^{(T)}$ and $D^{(S)}$ are the similarity matrix of $f^{(T)}$ and $f^{(S)}$, respectively.

However, the teacher model cannot learn sufficient knowledge from the training data in early epochs of training but becomes increasingly reliable as the epoch grows. Considering this, we use a dynamic weight updating scheme [19] to change the weight of PSD loss online. The dynamic weight formulation is $\frac{t}{T}\lambda$, where λ is the final weight for distillation, t is the current epoch, and T is the total epoch of training. We find that this dynamic updating scheme can reach a better performance than static weight. Finally, we extend the typical DML with our PSD, whose final objective function is written as:

$$\mathcal{L} = L_{\text{DML}} + \tau^2 \frac{t}{T} \lambda L_{\text{PSD}}, \quad (2)$$

where L_{DML} is an arbitrary metric learning loss function and τ^2 is a balanced parameter often applied in

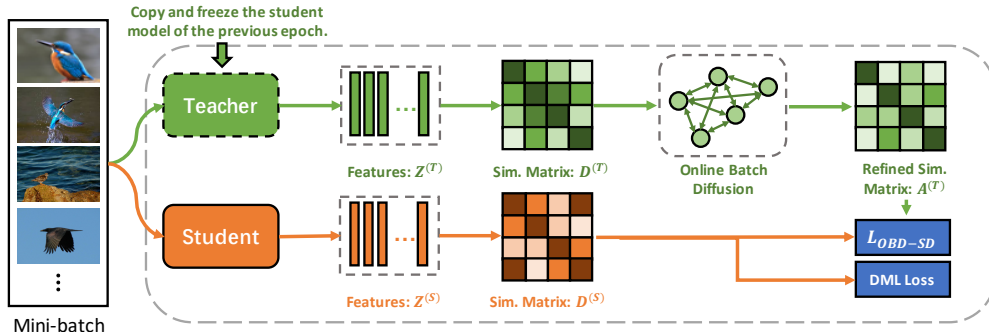


Figure 1: A schematic diagram of OBD-SD. The student trained in the previous epoch is the teacher in the current epoch. During the training, for each mini-batch, we use the teacher and the student models to produce the similarity matrices $D^{(T)}$ and $D^{(S)}$, respectively. Then, use online batch diffusion to refine $D^{(T)}$ to produce the refined similarity matrix $A^{(T)}$. Finally, compute DML losses while applying OBD-SD loss function on the matrices $A^{(T)}$ and $D^{(S)}$.

KD loss [13].

3.3 Online Batch Diffusion Process

However, there is another key problem in the PSD scheme, *i.e.*, the soft distance targets from the teacher model cannot fully reflect the intrinsic relationships among samples, because of the limitation of the rigid distance metrics [1, 51]. To solve this problem, we proposed Online Batch Diffusion Process (OBDDP) for refining the soft distance targets from the teacher model. OBDDP can help the embedding space learn more about intrinsic relationships among samples and improve performance.

3.3.1 Preliminaries of Diffusion Process

We first revisit the standard diffusion process in image retrieval (mainly following the steps from [59, 51]). Given a data set $\mathcal{U} = \{u_1, \dots, u_q, u_{q+1}, \dots, u_n\}$, the first q samples are the queries and the rest are the gallery. We define $\mathbf{f}^0 = [\mathbf{f}_1^0, \dots, \mathbf{f}_n^0]^T$, in which $\mathbf{f}_i^0 = 1$ if u_i is a query and $\mathbf{f}_i^0 = 0$ otherwise. The typical diffusion process has three steps, which can be described as follows:

1. Use a pre-trained model to extract the features $\mathcal{Z} = \{z_1, \dots, z_n\}$ from dataset \mathcal{U} and calculate

the affinity matrix $W \in \mathbb{R}^{n \times n}$, where each component $W_{ij} = d(z_i, z_j)$. Note that $W_{ii} = 0$ because there are no loops in the graph.

2. Symmetrically normalize W by $S = V^{-1/2} W V^{-1/2} \in \mathbb{R}^{n \times n}$, in which $V \in \mathbb{R}^{n \times n}$ is the diagonal matrix with $V_{ii} = \sum_{j=1}^n W_{ij}$. We refer to S as transition matrix.
3. Use random walk to iterate $\mathbf{f}^{t+1} = \omega S \mathbf{f}^t + (1 - \omega) \mathbf{f}^0$ until convergence, where $\omega \in (0, 1)$ is the transition probability of random walk.

It can be proved that the above iteration converges to a closed-form solution:

$$\mathbf{f}^\infty = (1 - \omega)(I - \omega S)^{-1} \mathbf{f}^0 \in \mathbb{R}^n. \quad (3)$$

where \mathbf{f}^∞ can be used as ranking scores for re-ranking.

3.3.2 Online Diffusion on Batch Manifolds

The standard diffusion process is commonly used as a re-ranking method. Though the Eq 3 requires $O(N^3)$ time complexity (N is the number of samples), we only need to compute it once offline. However, if we want to use diffusion process during training, we

need to update and maintain the Eq 3 online, which is impractical since the size of the training set is large.

To solve this problem, we proposed Online Batch Diffusion Process (OBDP), in which we only use the samples in the mini-batch to construct the neighborhood graph for diffusion process each time. This means that we only diffuse information on batch manifolds. Specifically, for each mini-batch \mathcal{B} , we first use a teacher model to extract the features $\mathcal{Z}^{(T)} \in \mathbb{R}^{|\mathcal{B}| \times d}$ and then calculate the similarity matrix $D \in \mathbb{R}^{|\mathcal{B}| \times |\mathcal{B}|}$. Note that since our aim is to refine relationships between samples rather than simply calculate ranking scores, we use D as the initial state for diffusion in OBDP, which is different from the standard diffusion process. Then we calculate the affinity matrix $W \in \mathbb{R}^{|\mathcal{B}| \times |\mathcal{B}|}$ and transition matrix $S \in \mathbb{R}^{|\mathcal{B}| \times |\mathcal{B}|}$ based on the extracted $\mathcal{Z}^{(T)}$. Finally, we use random walk to refine the initial states D :

$$A = (1 - \omega)(I - \omega S)^{-1}D \in \mathbb{R}^{|\mathcal{B}| \times |\mathcal{B}|}, \quad \omega \in (0, 1) \quad (4)$$

where A is the refined similarity matrix of the mini-batch \mathcal{B} . Since $|\mathcal{B}|$ is usually much smaller than the size of training set N , OBDP can be efficiently computed online. Moreover, if $|\mathcal{B}|$ is fixed, Eq 4 only requires $O(N)$ for each epoch, which is more efficient than the standard diffusion process.

3.4 Online Batch Diffusion-based Self-distillation

Now, we can use OBDP to refine the soft distance targets from PSD. Specifically, for each mini-batch \mathcal{B} , we use the teacher model $f^{(T)}$ to extract the features $\mathcal{Z}^{(T)}$ and apply OBDP to calculate the refined similarity matrix $A^{(T)}$:

$$A^{(T)} = (1 - \omega)(I - \omega S^{(T)})^{-1}D^{(T)}, \quad (5)$$

where the similarity matrix $D^{(T)}$ and transition matrix $S^{(T)}$ are both calculated by using $\mathcal{Z}^{(T)}$. Then, we replace $D^{(T)}$ in Eq 1 with $A^{(T)}$. Thus our OBD-SD loss is:

$$L_{\text{OBD-SD}}(\mathcal{B}) = \frac{1}{|\mathcal{B}|} \sum_{i=1}^{|\mathcal{B}|} \sum_{j=1}^{|\mathcal{B}|} \sigma(A_{i,:}^{(T)}/\tau)_j \ln \frac{\sigma(A_{i,:}^{(T)}/\tau)_j}{\sigma(D_{i,:}^{(S)}/\tau)_j}, \quad (6)$$

Overall, the final objective function can be described as:

$$\mathcal{L} = L_{\text{DML}} + \tau^2 \frac{t}{T} \lambda L_{\text{OBD-SD}}, \quad (7)$$

4 Theoretical Support

In this section, we show why OBD-SD can improve metric learning. We analyze PSD and OBDP, respectively¹.

4.1 Analysis for PSD

We analyze the gradients of PSD. First, the gradient for L_{PSD} (for convenience, L_{PSD} here is for an anchor \mathbf{x}_i) *w.r.t.* the embedded feature \mathbf{v}_i is:

$$\frac{\partial L_{\text{PSD}}}{\partial \mathbf{v}_i} = \sum_j^{|\mathcal{B}|} (\mathbf{z}_j - (\mathbf{z}_i \cdot \mathbf{z}_j) \mathbf{z}_i) (P_{ij} - S_{ij}), \quad (8)$$

where P_{ij} and S_{ij} are the relationships between \mathbf{x}_i and \mathbf{x}_j predicted by the student and teacher, respectively. We can observe that Eq 8 contains two parts: ‘‘attention part’’ ($\mathbf{z}_j - (\mathbf{z}_i \cdot \mathbf{z}_j) \mathbf{z}_i$) and ‘‘difference part’’ ($P_{ij} - S_{ij}$).

First, we analyze the ‘‘attention part’’. Take positive samples as an example, for an easy positive sample $\mathbf{z}_i \cdot \mathbf{z}_j \approx 1$, we can achieve:

$$\|\mathbf{z}_p - (\mathbf{z}_i \cdot \mathbf{z}_p) \mathbf{z}_i\| = \sqrt{1 - (\mathbf{z}_i \cdot \mathbf{z}_p)^2} \approx 0, \quad (9)$$

And for an hard positive sample $0 < \mathbf{z}_i \cdot \mathbf{z}_p \ll 1$, we have:

$$\|\mathbf{z}_p - (\mathbf{z}_i \cdot \mathbf{z}_p) \mathbf{z}_i\| = \sqrt{1 - (\mathbf{z}_i \cdot \mathbf{z}_p)^2} \approx 1, \quad (10)$$

Obviously, for easy samples, the gradient of L_{PSD} along \mathbf{v}_i is close to 0, while for hard samples is equal to $\|\mathbf{z}_p - (\mathbf{z}_i \cdot \mathbf{z}_p) \mathbf{z}_i\| |P_{ip} - S_{ip}| \approx |P_{ip} - S_{ip}|$. This shows that the gradient contribution of easy samples is relatively small while the gradient contribution of hard samples is large. This result implies that PSD encourages the model to pay more attention to hard

¹We provide the full derivation in Section S.4 of the supplementary.

samples during training. We argue that there is usually more intrinsic information (such as intra-class variations) in hard samples that conventional methods would suppress.

Second, we analyze the “difference part”. The “difference part” shows that PSD forces the student’s output P_{ip} to become similar to the teacher’s S_{ip} , rather than leverage solely class labels to increase inter-class distances and decrease intra-class distances. Hence, the student can learn more information in the process of imitation, especially for hard samples, thus alleviating the problem of ignoring the intrinsic relationships of samples.

4.2 Analysis for OBDP

Inspired by [2, 1], our OBDP can be seen as the following optimization problem:

$$\begin{aligned} \min_A \frac{1}{2} \sum_{i,j,k=1}^{|\mathcal{B}|} W_{j,k} \left(\frac{A_{i,j}}{\sqrt{V_{i,i}V_{j,j}}} - \frac{A_{i,k}}{\sqrt{V_{i,i}V_{k,k}}} \right)^2 \\ + \frac{1-\omega}{\omega} \sum_{i,j=1}^{|\mathcal{B}|} (A_{i,j} - D_{i,j})^2 \end{aligned} \quad (11)$$

where A represents the refined similarity and D is the initial similarity matrix. Eq. 11 consists of two terms. From the first term, we can find that OBDP takes into account high-order relationship information between samples. For example, the relationships between \mathbf{x}_i and \mathbf{x}_j (denoted by $A_{i,j}$) is interrelated to relationship between \mathbf{x}_i and all other samples in the batch (denoted by $A_{i,k}, k = 1, \dots, |\mathcal{B}|$) with weights $W_{j,k}$. In contrast, $D_{i,j}$ only considers pairwise relationships on rigid distance metrics and ignores the intrinsic relationships between samples. We infer that such high-order information on batch manifolds can help the embedding space better reveal the intrinsic relationships between objects as the high-order information on the global manifolds does [5]. The second term suggests that the initial states should be preserved to a certain extent. It emphasizes that a good distance measurement should not differ too much from the initial states.

5 Experiments

5.1 Experimental Details

Datasets. To evaluate the generalization on unseen classes, we followed the existing experiment setting from [35, 34], which is a zero-shot setting where the training set has no intersection with the test set. We conduct experiments on three benchmark dataset, such as **CUB200-2011** [44], **CARS196** [23] and **Stanford Online Products (SOP)** [28]. The CUB200-2011 contains 11,788 images of 200 classes of birds. We use the first/last 100 classes (5,864/5,924 images respectively) as the training/test subsets. The CARS196 contains 16,185 images of 196 car categories. We use the first/last 98 classes (8,054/8,131 images) as the training/test subsets. The SOP contains 120,053 online product images in 22,634 categories. We use the first 11,318 classes of 59,551 images as the training subset and the remaining 11,316 classes of 60,502 images as the test subset.

Evaluation Metrics. Recall@K (R@K) [17] and Normalized Mutual Information (NMI) [25] are used, where R@k measures the image retrieval performance while NMI measures the image clustering performance. Please see the supplementary (Section S.1) for more information.

Implementation Details. We utilize a ImageNet pretrained ResNet50 (R50/d) or Inception BN (IBN/d) with frozen Batch-Normalization layers as the backbone network, where the d is the embedding dimension. If not specifically emphasized, we use R50/128 by default in experiments. We use Adam optimizer with a fixed learning rate of 10^{-5} and a weight decay of 4×10^{-4} . Note that there is no learning rate scheduling for unbiased comparison, if not mentioned. We set the distillation weight λ /transition probability ω to 1000/0.3 for CUB200-2011, 75/0.99 for CARS196 and 100/0.5 for Stanford Online Products, and the temperature to 1 by default. Each training was run over 150 epochs for CUB200-2011/CARS196 and 100 epochs for Stanford Online Products. All experiments were performed on a single Nvidia V100 GPU and all results are computed over multiple seeds averages. Additional details are available in the supplementary (Section S.3).

Table 1: Comparison with strong metric learning baselines. **Bold** denotes the better result between using OBD-SD and not using OBD-SD with the same metric learning loss function.

Benchmarks→	CUB200-2011		CARS196		SOP	
Approaches↓	R@1	NMI	R@1	NMI	R@1	NMI
Margin ($\beta = 1.2$) [49]	63.15	68.05	80.02	67.50	78.20	90.32
Margin ($\beta = 1.2$) + OBD-SD (Ours)	65.78 (\uparrow 2.63)	69.67 (\uparrow 1.62)	81.49 (\uparrow 1.47)	68.18 (\uparrow 0.68)	78.81 (\uparrow 0.61)	90.51 (\uparrow 0.19)
R-Margin ($\beta = 0.6$) [35]	64.54	68.31	82.39	68.57	77.45	90.36
R-Margin ($\beta = 0.6$) + OBD-SD (Ours)	66.54 (\uparrow 2.00)	69.24 (\uparrow 0.93)	84.49 (\uparrow 2.10)	70.24 (\uparrow 1.67)	77.75 (\uparrow 0.30)	90.50 (\uparrow 0.14)
MS [46]	63.10	68.33	81.56	69.38	77.75	90.01
MS + OBD-SD (Ours)	67.76 (\uparrow 4.66)	70.81 (\uparrow 2.48)	84.10 (\uparrow 2.54)	70.93 (\uparrow 1.55)	78.83 (\uparrow 1.08)	90.22 (\uparrow 0.21)

Table 2: Comparison with state-of-the-art metric learning methods across different Architecture (Arch) and Dimensionality (Dim). “+D” indicates that use combinational pooling in backbone as done in [20]. **Bold** denotes the best result in the given Arch/Dim setting. **Blue** indicates the best results overall.

Benchmarks→	CUB200-2011			CARS196			SOP				
Approaches↓	Venue	Arch/Dim	R@1	R@2	NMI	R@1	R@2	NMI	R@1	R@10	NMI
Div&Conq [37]	CVPR’19	R50/128	65.9	76.6	69.6	84.6	90.7	70.3	75.9	88.4	90.2
MIC [32]	ICCV’19	R50/128	66.1	76.8	69.7	82.6	89.1	68.4	77.2	89.4	90.0
PADS [33]	CVPR’20	R50/128	67.3	78.0	69.9	83.5	89.7	68.8	76.5	89.0	89.9
RankMI [18]	CVPR’20	R50/128	66.7	77.2	71.3	83.3	89.8	69.4	74.3	87.9	90.5
MS+PLG [36] ²	CVPR’22	R50/128	67.8	78.2	70.1	86.0	91.4	72.4	77.9	89.9	90.2
MS + OBD-SD (Ours)	-	R50/128	67.8	78.1	70.8	84.9	91.0	72.1	79.6	91.2	90.4
	-	R50/128+D	68.0	78.3	71.1	86.2	91.6	73.1	79.6	91.2	90.3
ProxyAnchor (PA) [20]	CVPR’20	IBN/512+D	68.4	79.2	-	86.1	91.6	-	79.1	90.8	-
ProxyGML [60]	NeurIPS’20	IBN/512	66.7	77.6	69.8	85.5	91.8	72.4	78.0	90.6	90.4
PA+DRML [57]	ICCV’21	IBN/512	68.7	78.6	69.3	86.9	92.1	72.1	71.5	85.2	88.1
PA+MemVir [22]	ICCV’21	IBN/512	69.0	79.2	-	86.7	92.0	-	79.7	91.0	-
EPSHN [50]	WACV’20	R50/512	64.9	75.3	-	82.7	89.3	-	78.3	90.7	-
DiVA [26]	ECCV’20	R50/512	69.2	79.3	71.4	87.6	92.9	72.2	79.6	91.2	90.6
DCML-MDW [56]	CVPR’21	R50/512	68.4	77.9	71.8	85.2	91.8	73.9	79.8	90.8	90.8
MS+DAS [24]	ECCV’22	R50/512+D	69.2	79.3	-	87.8	93.1	-	80.6	91.8	-
MS + OBD-SD (Ours)	-	IBN/512	65.8	76.8	68.8	85.4	91.4	70.4	77.6	90.0	89.6
	-	IBN/512+D	65.8	76.9	68.7	85.8	92.1	71.6	77.9	90.1	89.5
	-	R50/512	69.1	79.5	71.1	86.5	92.3	72.0	80.7	92.0	90.4
	-	R50/512+D	69.4	79.7	71.4	88.7	93.6	74.5	81.0	92.1	90.1

5.2 Effectiveness of OBD-SD

To validate the effectiveness, we use R50/128 as the backbone. We select three methods that can achieve top-3 performance evaluated in [35], *i.e.*, Multisimilarity (MS) loss [46], Margin loss with Distance-based Sampling [49] and Regularized Margin loss [35], and follow their experimental training pipeline. Note that the setup utilizes no learning rate scheduling and fixes common implementational factors of variation (such as batch-size) in DML pipelines to ensure comparability. The results are presented in Table 1, which shows that our OBD-SD improves the original DML approaches on all benchmarks.

To further highlight the benefits, we compare our

OBD-SD with other state-of-the-art methods and report results in Table 2. The compared methods can be divided into different groups (*i.e.*, R50/128, R50/512 and IBN/512), according to their backbone and embedding dimensions. Note that we apply learning rate scheduling and extend the number of the training epoch appropriately. The results in Table 1 show that OBD-SD can achieve competitive performance across different architectures and benchmarks.

5.3 Ablation Studies

Ablation study of each element. We perform ablation studies to evaluate the effectiveness of each

Table 3: Ablation study using different elements of OBD-SD.

Datasets→	CUB200-2011		CARS196	
Methods↓	R@1	NMI	R@1	NMI
MS [46]	63.1	68.3	81.6	69.4
+ PSD w/o dynamic weight	62.9	68.6	81.9	69.4
+ PSD	63.5	69.1	82.3	70.0
+ OBD-SD (PSD+OBDP)	67.8	70.8	84.1	70.9

Table 4: Ablation studies on different sampling strategies. The suffixes ‘(R)’, ‘(H)’, ‘(S)’ and ‘(D)’ denote the random, semi-hard, soft-hard and distance-based sampling strategy, respectively.

Datasets→	CUB200-2011		CARS196	
Methods↓	R@1	NMI	R@1	NMI
Margin (R)	55.5	61.7	66.1	59.5
+ OBD-SD	62.3	67.1	73.3	63.1
Margin (H) [38]	61.2	66.5	76.1	64.4
+ OBD-SD	63.6	67.8	78.3	65.6
Margin (S) [32]	61.3	66.5	77.7	66.1
+ OBD-SD	63.3	68.1	78.6	66.4
Margin (D) [49]	63.2	68.1	80.0	67.5
+ OBD-SD	65.8	69.7	81.5	68.2

element in OBD-SD. We use MS loss as the default DML loss. The results are shown in Table 3. We observe that our OBD-SD (PSD with OBDP) achieves the best result, demonstrating the effectiveness of each proposed element. For the “+PSD w/o dynamic weight”, we conduct ablation experiments to select the best λ value.

Ablation Studies on Different Sampling Strategies. Data sampling is an important technique for pair-based DML methods. To analyze the impact of data sampling on OBD-SD, we employ four popular data sampling strategies: 1) random sampling, 2) semi-hard sampling [38], 3) soft-hard mining [32], and 4) distance-based tuple mining [49] with Margin loss [49] for the experiments. We report the results in Table 4. We find that OBD-SD can consistently improve performance through different sampling strategies.

²Require pretrained natural language models.

Table 5: Comparison with other self-distillation methods of DML.

Datasets→	CUB200-2011			CARS196		
Methods↓	R@1	NMI	GPU-Time	R@1	NMI	GPU-Time
MS [46]	63.1	68.3	-	81.6	69.4	-
MS+BAR [30]	64.1	68.4	+105.3%	82.6	69.6	+101.9%
MS+PSD (Ours)	63.5	69.1	+5.3%	82.3	70.0	+1.9%
MS+S2SD-MSD [34] ³	65.2	70.6	+50.4%	84.0	71.3	+35.4%
MS+OBD-SD (Ours)	67.8	70.8	+17.4%	84.1	70.9	+7.4%

5.4 Comparison with Self-KD of DML.

Then, we compare OBD-SD with recently proposed Self-KD-based DML methods, such as BAR [30] and S2SD [34]. We use MS loss as the basic DML loss for all experiments in this part. For BAR, we select the best distillation weights by ablation experiments (100/50 for CUB200/CARS196) since the paper doesn’t show the experiments on the datasets we used, and for S2SD, we follow the setting of its paper. The results are shown in Table 5. Compared with BAR, our proposed Self-KD method, PSD, can achieve competitive results with only 5.3% and 1.9% extra training time on CUB200 and CARS196 datasets, while BAR requires almost double training time. We also compare OBD-SD with S2SD, a SOTA Self-KD method for DML. The results in Table 5 show that our OBD-SD requires much less extra training time, 17.4% and 7.4% on the two datasets, and achieves competitive performance.

Since our OBDP is a plug-and-play technique, we combine OBDP with recent Self-KD-based DML, *i.e.*, BAR and S2SD, to study the benefits of OBDP. Specifically, similar to our OBD-SD, we use OBDP to refine the soft labels generated by teachers (in BAR and S2SD), then use the refined soft labels for knowledge distillation. The results are reported in Table 6, which shows that OBDP can also improve the performance of other Self-KD methods.

³We carefully reproduce the experiments by using the official code.

Table 6: Experimental results of applying OBDP to other self-distillation of methods of DML.

Datasets→	CUB200-2011		CARS196	
Methods↓	R@1	NMI	R@1	NMI
MS+BAR [30]	64.1	68.4	82.6	69.6
MS+BAR+OBDP	66.7	70.2	84.5	71.4
MS+S2SD-MSD [34]	65.2	70.6	84.0	71.3
MS+S2SD-MSD+OBDP	65.8	70.9	84.6	71.9

5.5 Batch Manifolds versus Global Manifolds

In this section, we conduct experiments comparing the diffusion in batch manifolds and in global manifolds. We use batch diffusion and global diffusion (Section 3.3.1) for refining the soft distance targets, respectively. As mentioned in Section 3.3, Eq. 3 requires $O(N^3)$ time complexity, so it’s impossible for us to update it for each mini-batch (online diffusion). Instead, in our experiments, we update the matrix once after each training epoch (offline diffusion). Specifically, after the training of each epoch, we use the new teacher to extract features of the training set and calculate the refined similarity matrix for all data. When we train the student in the next epoch, for each batch, we select the related elements from the refined similarity matrix for knowledge distillation. Note that this strategy leads to ignoring some variation factors, such as those caused by data augmentations. In addition, to reduce the space complexity and the noise from negative pairs, we construct the affinity matrix W as follows:

$$W_{i,j} = \begin{cases} d(\mathbf{z}_i, \mathbf{z}_j) & i \neq j, \mathbf{x}_i \in \text{NN}_k(\mathbf{x}_j), \mathbf{x}_j \in \text{NN}_k(\mathbf{x}_i) \\ 0 & \text{otherwise} \end{cases} \quad (12)$$

where $\text{NN}_k(\mathbf{z})$ denotes the top- k nearest samples of \mathbf{x} . This way can also improve the speed of diffusion. In our experiments, we set $k = 50$ and use MS loss, the size of the training set for CUB200 and CARS196 datasets are 5,864 and 8,054 respectively, and the size of the mini-batch is 112. The results are reported in Table 7. From the results, we can find that diffusion in batch manifold can achieve almost the same result as diffusion in global manifold and

Table 7: The results of “Batch Manifolds vs Global Manifolds”.

Datasets→	CUB200-2011			CARS196		
Methods↓	R@1	NMI	GPU-Time	R@1	NMI	GPU-Time
In global manifold	67.3	70.6	+248.8%	84.4	71.0	+345.0%
In batch manifold (Ours)	67.8	70.8	+17.4%	84.1	70.9	+7.4%

with much less extra time.

5.6 Embedding Space Metrics

We investigate the effect of OBD-SD on embedding space. We observe the differences between the embedding space learned with and without OBD-SD by using different structural measurements. (1) *Embedding Space Density* [35]: $\pi_{\text{ratio}}(\Phi) = \pi_{\text{intra}}(\Phi)/\pi_{\text{inter}}(\Phi)$, which measures the ratio of mean inter-class distances $\pi_{\text{inter}}(\Phi)$ and mean intra-class distances $\pi_{\text{intra}}(\Phi)$. Note that the higher value of embedding space density indicates lower class concentration and is linked to stronger generalization. (2) *Spectral Decay* [35]: $\rho(\Phi) = \text{KL}(\mathcal{U}||S(\Phi))$, where $\rho(\Phi)$ calculates the KL-divergence between uniform distribution \mathcal{U} and singular value decomposition $S(\Phi)$ of embedding space Φ . The spectral decay measures the number of directions of significant variance in the learned embedding space. Note that the lower value of spectral decay indicates high feature variety and is linked to stronger generalization. In our experiments, we exclude the two largest spectral values for a more robust estimate. Please see the supplementary (Section S.2) for more information.

The experimental results are reported in Table 8. The results show that both PSD and OBDP improve the embedding space density and reduce the spectral decay, linked to more robust generalization as described above. In other words, OBD-SD can reduce the over-clustering in the embedding space and increase embedding representation diversity, which means OBD-SD can encourage the model to find more intrinsic relation information. The result is consistent with our initial motivation for OBD-SD.

Table 8: Results of embedding space density $\pi_{\text{ratio}}(\Phi)$ and spectral decay $\rho(\Phi)$.

Datasets→	CUB200-2011		CARS196	
Methods↓	$\pi_{\text{ratio}}(\Phi)$	$\rho(\Phi)$	$\pi_{\text{ratio}}(\Phi)$	$\rho(\Phi)$
MS	0.4427	0.1544	0.3962	0.1622
MS+PSD	0.4504↑	0.1444↓	0.4256↑	0.1496↓
MS+OBD-SD	0.6291↑	0.0292↓	0.7083↑	0.0264↓

5.7 Robustness to Mislabeled Data

Since our approach alleviates the constraints imposed by sample annotation, a natural question is raised: *Does it also improve the robustness to mislabeled data?*

To answer this question, we generate mislabeled data on the three datasets (CUB200, CARS196 and Stanford Online Products) with $\{0.1, 0.2, 0.3, 0.4\}$ symmetric mislabeled ratios, following [11] and [43]. We then use MS loss as the baseline and train models on the mislabeled data with and without OBD-SD. The results in Table 9 indicate that OBD-SD consistently achieves performance promotions on mislabeled training data. Moreover, we calculate the percentage of improvement relative to the baseline for each metric as follows: $P_{\text{metric}} = (V_{SD} - V_{\text{base}}) / V_{\text{base}}$, where V_{SD} and V_{base} are the value of the metric for OBD-SD and the baseline, respectively. We can find that the performance promotions become more pronounced as the mislabeled ratio increases. This result shows that OBD-SD can improve the robustness to mislabeled data.

6 Conclusion

In this paper, we propose Online Batch Diffusion-based Self-distillation (OBD-SD) to alleviate the "ignore intrinsic relation" issue of DML methods. To this end, we propose Progressive Self-distillation (PSD) to encourage the model to learn more relational information among samples. Then, we further propose Online Batch Diffusion Process (OBDP) to help PSD reveal the intrinsic relationships among samples on batch manifolds. Extensive experiments with various loss functions on three benchmarks show

Table 9: Results on the three datasets validation with different noisy ratios on the training sets.

Noisy ratio	Benchmarks→ Approaches↓	CUB200		CARS196	
		R@1	NMI	R@1	NMI
0.1	MS	59.69	66.70	76.81	65.26
	MS+OBD-SD	66.11 (+10.75%)	69.93 (+4.84%)	80.47 (+4.77%)	67.85 (+3.97%)
0.2	MS	55.83	63.92	71.33	60.92
	MS+OBD-SD	64.23 (+15.05%)	68.84 (+7.70%)	76.57 (+7.35%)	65.09 (+6.85%)
0.3	MS	52.03	61.06	66.53	56.24
	MS+OBD-SD	61.83 (+18.84%)	67.00 (+9.73%)	71.16 (+6.96%)	59.98 (+6.65%)
0.4	MS	48.25	57.75	60.97	51.16
	MS+OBD-SD	58.11 (+20.44%)	65.05 (+13.07%)	65.58 (+7.56%)	54.43 (+6.39%)

that OBD-SD is effective and efficient. However, our proposed method can't consistently improve the performance of proxy-based DML, which is a strong method of DML. In the future, we plan to explore the diffusion process on the proxies-manifold for optimizing the embedding space for proxy-based DML. In addition, we also plan to apply OBD-SD to other areas such as self-supervised learning

7 Supplemental Material

You can download the Supplemental Material from https://github.com/ZelongZeng/OBD-SD_Pytorch.

8 Acknowledgements

This research is part of the results of Value Exchange Engineering, a joint research project between Mercari, Inc. and the RIISE of the University of Tokyo.

References

- [1] Song Bai, Xiang Bai, Qi Tian, and Longin Jan Latecki. Regularized diffusion process for visual retrieval. In *Proceedings of the AAAI Conference on Artificial Intelligence*, volume 31, 2017. 2, 3, 5, 7
- [2] Song Bai, Zhichao Zhou, Jingdong Wang, Xiang Bai, Longin Jan Latecki, and Qi Tian. Ensemble diffusion for retrieval. In *Proceedings of the IEEE Interna-*

- tional conference on computer vision*, pages 774–783, 2017. 7
- [3] Andrew Brown, Weidi Xie, Vicky Kalogeiton, and Andrew Zisserman. Smooth-ap: Smoothing the path towards large-scale image retrieval. In *European Conference on Computer Vision*, pages 677–694. Springer, 2020. 3
- [4] Jiankang Deng, Jia Guo, Niannan Xue, and Stefanos Zafeiriou. Arcface: Additive angular margin loss for deep face recognition. In *Proceedings of the IEEE/CVF Conference on Computer Vision and Pattern Recognition*, pages 4690–4699, 2019. 1
- [5] Michael Donoser and Horst Bischof. Diffusion processes for retrieval revisited. In *Proceedings of the IEEE conference on computer vision and pattern recognition*, pages 1320–1327, 2013. 3, 7
- [6] Tommaso Furlanello, Zachary Lipton, Michael Tschannen, Laurent Itti, and Anima Anandkumar. Born again neural networks. In *International Conference on Machine Learning*, pages 1607–1616. PMLR, 2018. 2, 3, 4
- [7] Weifeng Ge. Deep metric learning with hierarchical triplet loss. In *Proceedings of the European Conference on Computer Vision (ECCV)*, pages 269–285, 2018. 3
- [8] Albert Gordo, Jon Almazán, Jerome Revaud, and Diane Larlus. Deep image retrieval: Learning global representations for image search. In *European conference on computer vision*, pages 241–257. Springer, 2016. 1
- [9] Albert Gordo, Jon Almazan, Jerome Revaud, and Diane Larlus. End-to-end learning of deep visual representations for image retrieval. *International Journal of Computer Vision*, 124(2):237–254, 2017. 1
- [10] Raia Hadsell, Sumit Chopra, and Yann LeCun. Dimensionality reduction by learning an invariant mapping. In *2006 IEEE Computer Society Conference on Computer Vision and Pattern Recognition (CVPR’06)*, volume 2, pages 1735–1742. IEEE, 2006. 3
- [11] Bo Han, Quanming Yao, Xingrui Yu, Gang Niu, Miao Xu, Weihua Hu, Ivor Tsang, and Masashi Sugiyama. Co-teaching: Robust training of deep neural networks with extremely noisy labels. *arXiv preprint arXiv:1804.06872*, 2018. 11
- [12] Alexander Hermans, Lucas Beyler, and Bastian Leibe. In defense of the triplet loss for person re-identification. *arXiv preprint arXiv:1703.07737*, 2017. 1
- [13] Geoffrey Hinton, Oriol Vinyals, and Jeff Dean. Distilling the knowledge in a neural network. *arXiv preprint arXiv:1503.02531*, 2015. 3, 5
- [14] Qian Huang, Horace He, Abhay Singh, Ser-Nam Lim, and Austin R Benson. Combining label propagation and simple models out-performs graph neural networks. *arXiv preprint arXiv:2010.13993*, 2020. 3
- [15] Ahmet Iscen, Giorgos Tolias, Yannis Avrithis, and Ondrej Chum. Label propagation for deep semi-supervised learning. In *Proceedings of the IEEE/CVF Conference on Computer Vision and Pattern Recognition*, pages 5070–5079, 2019. 3
- [16] Ahmet Iscen, Giorgos Tolias, Yannis Avrithis, Teddy Furon, and Ondrej Chum. Efficient diffusion on region manifolds: Recovering small objects with compact cnn representations. In *Proceedings of the IEEE conference on computer vision and pattern recognition*, pages 2077–2086, 2017. 3
- [17] Herve Jegou, Matthijs Douze, and Cordelia Schmid. Product quantization for nearest neighbor search. *IEEE transactions on pattern analysis and machine intelligence*, 33(1):117–128, 2010. 7
- [18] Mete Kemertas, Leila Pishdad, Konstantinos G Derpanis, and Afsaneh Fazly. Rankmi: A mutual information maximizing ranking loss. In *Proceedings of the IEEE/CVF Conference on Computer Vision and Pattern Recognition*, pages 14362–14371, 2020. 8
- [19] Kyungyul Kim, ByeongMoon Ji, Doyoung Yoon, and Sangheum Hwang. Self-knowledge distillation with progressive refinement of targets. In *Proceedings of the IEEE/CVF International Conference on Computer Vision*, pages 6567–6576, 2021. 2, 3, 4
- [20] Sungyeon Kim, Dongwon Kim, Minsu Cho, and Suha Kwak. Proxy anchor loss for deep metric learning. In *Proceedings of the IEEE/CVF Conference on Computer Vision and Pattern Recognition*, pages 3238–3247, 2020. 3, 8
- [21] Sungyeon Kim, Dongwon Kim, Minsu Cho, and Suha Kwak. Embedding transfer with label relaxation for improved metric learning. In *Proceedings of the IEEE/CVF Conference on Computer Vision and Pattern Recognition*, pages 3967–3976, 2021. 3, 4
- [22] Byungsoo Ko, Geonmo Gu, and Han-Gyu Kim. Learning with memory-based virtual classes for deep metric learning. In *Proceedings of the IEEE/CVF International Conference on Computer Vision*, pages 11792–11801, 2021. 8
- [23] Jonathan Krause, Michael Stark, Jia Deng, and Li Fei-Fei. 3d object representations for fine-grained

- categorization. In *Proceedings of the IEEE international conference on computer vision workshops*, pages 554–561, 2013. **2, 7**
- [24] Lizhao Liu, Shangxin Huang, Zhuangwei Zhuang, Ran Yang, Mingkui Tan, and Yaowei Wang. Das: Densely-anchored sampling for deep metric learning. *arXiv preprint arXiv:2208.00119*, 2022. **8**
- [25] Christopher D Manning. *Introduction to information retrieval*. Synpress Publishing,, 2008. **7**
- [26] Timo Milbich, Karsten Roth, Homanga Bharadhwaj, Samarth Sinha, Yoshua Bengio, Björn Ommer, and Joseph Paul Cohen. Diva: Diverse visual feature aggregation for deep metric learning. In *European Conference on Computer Vision*, pages 590–607. Springer, 2020. **2, 3, 8**
- [27] Yair Movshovitz-Attias, Alexander Toshev, Thomas K Leung, Sergey Ioffe, and Saurabh Singh. No fuss distance metric learning using proxies. In *Proceedings of the IEEE International Conference on Computer Vision*, pages 360–368, 2017. **3**
- [28] Hyun Oh Song, Yu Xiang, Stefanie Jegelka, and Silvio Savarese. Deep metric learning via lifted structured feature embedding. In *Proceedings of the IEEE conference on computer vision and pattern recognition*, pages 4004–4012, 2016. **2, 3, 7**
- [29] Qi Qian, Lei Shang, Baigui Sun, Juhua Hu, Hao Li, and Rong Jin. Softtriple loss: Deep metric learning without triplet sampling. In *Proceedings of the IEEE/CVF International Conference on Computer Vision*, pages 6450–6458, 2019. **3**
- [30] Zhen Qin, Le Yan, Yi Tay, Honglei Zhuang, Xuanhui Wang, Michael Bendersky, and Marc Najork. Born again neural rankers. *arXiv preprint arXiv:2109.15285*, 2021. **3, 4, 9, 10**
- [31] Michal Rolinek, Vít Musil, Anselm Paulus, Marin Vlastelica, Claudio Michaelis, and Georg Martius. Optimizing rank-based metrics with blackbox differentiation. In *Proceedings of the IEEE/CVF Conference on Computer Vision and Pattern Recognition*, pages 7620–7630, 2020. **3**
- [32] Karsten Roth, Biagio Brattoli, and Bjorn Ommer. Mic: Mining interclass characteristics for improved metric learning. In *Proceedings of the IEEE/CVF International Conference on Computer Vision*, pages 8000–8009, 2019. **3, 8, 9**
- [33] Karsten Roth, Timo Milbich, and Bjorn Ommer. Pads: Policy-adapted sampling for visual similarity learning. In *Proceedings of the IEEE/CVF Conference on Computer Vision and Pattern Recognition*, pages 6568–6577, 2020. **3, 8**
- [34] Karsten Roth, Timo Milbich, Bjorn Ommer, Joseph Paul Cohen, and Marzyeh Ghassemi. Simultaneous similarity-based self-distillation for deep metric learning. In *International Conference on Machine Learning*, pages 9095–9106. PMLR, 2021. **2, 3, 4, 7, 9, 10**
- [35] Karsten Roth, Timo Milbich, Samarth Sinha, Prateek Gupta, Bjorn Ommer, and Joseph Paul Cohen. Revisiting training strategies and generalization performance in deep metric learning. In *International Conference on Machine Learning*, pages 8242–8252. PMLR, 2020. **2, 7, 8, 10**
- [36] Karsten Roth, Oriol Vinyals, and Zeynep Akata. Integrating language guidance into vision-based deep metric learning. In *Proceedings of the IEEE/CVF Conference on Computer Vision and Pattern Recognition*, pages 16177–16189, 2022. **8**
- [37] Artsiom Sanakoyeu, Vadim Tschernezki, Uta Buchler, and Bjorn Ommer. Divide and conquer the embedding space for metric learning. In *Proceedings of the IEEE/CVF Conference on Computer Vision and Pattern Recognition*, pages 471–480, 2019. **2, 3, 8**
- [38] Florian Schroff, Dmitry Kalenichenko, and James Philbin. Facenet: A unified embedding for face recognition and clustering. In *Proceedings of the IEEE conference on computer vision and pattern recognition*, pages 815–823, 2015. **1, 3, 9**
- [39] Shai Shalev-Shwartz and Shai Ben-David. *Understanding machine learning: From theory to algorithms*. Cambridge university press, 2014. **3**
- [40] Kihyuk Sohn. Improved deep metric learning with multi-class n-pair loss objective. In *Advances in neural information processing systems*, pages 1857–1865, 2016. **3**
- [41] Juan Luis Suárez, Salvador García, and Francisco Herrera. A tutorial on distance metric learning: Mathematical foundations, algorithms, experimental analysis, prospects and challenges. *Neurocomputing*, 425:300–322, 2021. **2**
- [42] Frederick Tung and Greg Mori. Similarity-preserving knowledge distillation. In *Proceedings of the IEEE/CVF International Conference on Computer Vision*, pages 1365–1374, 2019. **3**
- [43] Brendan Van Rooyen, Aditya Menon, and Robert C Williamson. Learning with symmetric label noise: The importance of being unhinged. *Advances in neural information processing systems*, 28, 2015. **11**

- [44] Catherine Wah, Steve Branson, Peter Welinder, Pietro Perona, and Serge Belongie. The caltech-ucsd birds-200-2011 dataset. 2011. [2](#), [7](#)
- [45] Jiang Wang, Yang Song, Thomas Leung, Chuck Rosenberg, Jingbin Wang, James Philbin, Bo Chen, and Ying Wu. Learning fine-grained image similarity with deep ranking. In *Proceedings of the IEEE conference on computer vision and pattern recognition*, pages 1386–1393, 2014. [3](#)
- [46] Xun Wang, Xintong Han, Weilin Huang, Dengke Dong, and Matthew R Scott. Multi-similarity loss with general pair weighting for deep metric learning. In *Proceedings of the IEEE/CVF Conference on Computer Vision and Pattern Recognition*, pages 5022–5030, 2019. [2](#), [8](#), [9](#)
- [47] Xun Wang, Haozhi Zhang, Weilin Huang, and Matthew R Scott. Cross-batch memory for embedding learning. In *Proceedings of the IEEE/CVF Conference on Computer Vision and Pattern Recognition*, pages 6388–6397, 2020. [1](#)
- [48] Zheng Wang, Ruimin Hu, Chao Liang, Yi Yu, Junjun Jiang, Mang Ye, Jun Chen, and Qingming Leng. Zero-shot person re-identification via cross-view consistency. *IEEE Transactions on Multimedia*, 18(2):260–272, 2015. [1](#)
- [49] Chao-Yuan Wu, R Manmatha, Alexander J Smola, and Philipp Krahenbuhl. Sampling matters in deep embedding learning. In *Proceedings of the IEEE International Conference on Computer Vision*, pages 2840–2848, 2017. [2](#), [3](#), [8](#), [9](#)
- [50] Hong Xuan, Abby Stylianou, and Robert Pless. Improved embeddings with easy positive triplet mining. In *Proceedings of the IEEE/CVF Winter Conference on Applications of Computer Vision*, pages 2474–2482, 2020. [2](#), [3](#), [8](#)
- [51] Fan Yang, Ryota Hinami, Yusuke Matsui, Steven Ly, and Shin’ichi Satoh. Efficient image retrieval via decoupling diffusion into online and offline processing. In *Proceedings of the AAAI Conference on Artificial Intelligence*, volume 33, pages 9087–9094, 2019. [2](#), [3](#), [5](#)
- [52] Li Yuan, Francis EH Tay, Guilin Li, Tao Wang, and Jiashi Feng. Revisiting knowledge distillation via label smoothing regularization. In *Proceedings of the IEEE/CVF Conference on Computer Vision and Pattern Recognition*, pages 3903–3911, 2020. [2](#), [3](#), [4](#)
- [53] Sukmin Yun, Jongjin Park, Kimin Lee, and Jinwoo Shin. Regularizing class-wise predictions via self-knowledge distillation. In *Proceedings of the IEEE/CVF conference on computer vision and pattern recognition*, pages 13876–13885, 2020. [2](#), [3](#)
- [54] Sergey Zagoruyko and Nikos Komodakis. Paying more attention to attention: Improving the performance of convolutional neural networks via attention transfer. *arXiv preprint arXiv:1612.03928*, 2016. [3](#)
- [55] Linfeng Zhang, Jiebo Song, Anni Gao, Jingwei Chen, Chenglong Bao, and Kaisheng Ma. Be your own teacher: Improve the performance of convolutional neural networks via self distillation. In *Proceedings of the IEEE/CVF International Conference on Computer Vision*, pages 3713–3722, 2019. [3](#)
- [56] Wenzhao Zheng, Chengkun Wang, Jiwen Lu, and Jie Zhou. Deep compositional metric learning. In *Proceedings of the IEEE/CVF Conference on Computer Vision and Pattern Recognition*, pages 9320–9329, 2021. [2](#), [3](#), [8](#)
- [57] Wenzhao Zheng, Borui Zhang, Jiwen Lu, and Jie Zhou. Deep relational metric learning. In *Proceedings of the IEEE/CVF International Conference on Computer Vision*, pages 12065–12074, 2021. [2](#), [3](#), [8](#)
- [58] Dengyong Zhou, Olivier Bousquet, Thomas Lal, Jason Weston, and Bernhard Schölkopf. Learning with local and global consistency. *Advances in neural information processing systems*, 16, 2003. [3](#)
- [59] Dengyong Zhou, Jason Weston, Arthur Gretton, Olivier Bousquet, and Bernhard Schölkopf. Ranking on data manifolds. *Advances in neural information processing systems*, 16, 2003. [2](#), [3](#), [5](#)
- [60] Yuehua Zhu, Muli Yang, Cheng Deng, and Wei Liu. Fewer is more: A deep graph metric learning perspective using fewer proxies. *Advances in Neural Information Processing Systems*, 33:17792–17803, 2020. [8](#)